MREX: The Mainz Radius Experiment

Prof. Dr. Concettina Sfienti
Institut für Kernphysik (KPh)
Johannes Gutenberg-Universität Mainz
Johann-Joachim-Becher-Weg 45
55128 Mainz
Tel.: +49 6131 39-25841
Fax: +49 6131 39-20850
Email: sfienti@uni-mainz.de

Executive Summary

The Equation of State (EoS) is a fundamental property of nuclear matter that describes the relationships between energy, pressure, temperature, density, and neutron-proton asymmetry. Despite being 18 orders of magnitude different in size, nuclei and neutron stars are governed by the same physics enshrined in the EoS. In particular, the neutron-skin thickness of heavy nuclei is strongly correlated to the poorly-known slope of the symmetry energy at saturation density. In spite of the mounting experimental effort to determine the neutron-skin thickness of heavy nuclei, a precise determination remains elusive.
The extraction of the neutron-skin thickness in parity-violation experiments is based on the measurement of the weak form factor at a single value of momentum transfer. Thus, some assumptions concerning the surface thickness have to be made in order to reliably extract the neutron-skin thickness. In addition, the puzzling observation of a zero transverse asymmetry in ^{208}Pb from the PREX collaboration is still a matter of debate both because of the implications for false asymmetries contributing substantially to the total systematic error of the neutron-skin measurement, and because of the apparent failing of the theoretical predictions of such contributions.
In view of the expected growing number of gravitational wave measurements of neutron star mergers from LIGO and Virgo, the new astronomical observations on neutron star radii of NICER, and the planning for the ultimate measurement of neutron-skin thickness at MESA, it becomes imperative to thoroughly investigate the methodology to extract the neutron skin from parity violation measurements. The goals of the of project will be:

1. **Transverse Asymmetry Measurements on ^{208}Pb**
   The beam-normal single spin asymmetry of ^{208}Pb will be measured at MAMI at two different beam energies in the energy regime of the future MESA accelerator.

2. **Determination of the Surface Thickness of ^{208}Pb**
   For the first time the surface thickness of ^{208}Pb will be determined in parity-violation electron scattering at MAMI. These data will remove the dominant model dependence in the method to extract the neutron-skin thickness from parity-violation experiments.

Project description

1 Starting Point

1.1 State of the art and preliminary work

Neutron stars are among the most fascinating astrophysical objects: they are the densest manifestations of massive objects in the universe known so far. The basic properties of neutron stars such as their mass, radius, and cooling behavior are determined by the nuclear Equation of State (EoS)

$$E(\rho, \delta) = E(\rho, 0) + S(\rho)\delta^2 \tag{1}$$

with $\delta = (\rho_n - \rho_p)/(\rho_n + \rho_p)$ the relative asymmetry parameter and $S(\rho)$ the symmetry energy, quantifying the energy cost of introducing a neutron-proton asymmetry into the system.
Despite being 18 orders of magnitude different in size, nuclei and neutron stars are governed by the same physics enshrined in the nuclear EoS. In fact the slope of the symmetry-energy term of the EoS at saturation density

$$L = 3\rho_0 (dS(\rho)/d\rho)_{\rho_0} \tag{2}$$

controls both the neutron-skin thickness in heavy nuclei and the radius of neutron stars [1].
The neutron-skin thickness of a nucleus is defined as the difference between the neutron and proton rms-radii. Because of its strong correlation with L (Fig. 1, left plot) [2], its accurate experimental determination would provide considerable constraints on the density dependence of the nuclear symmetry energy.

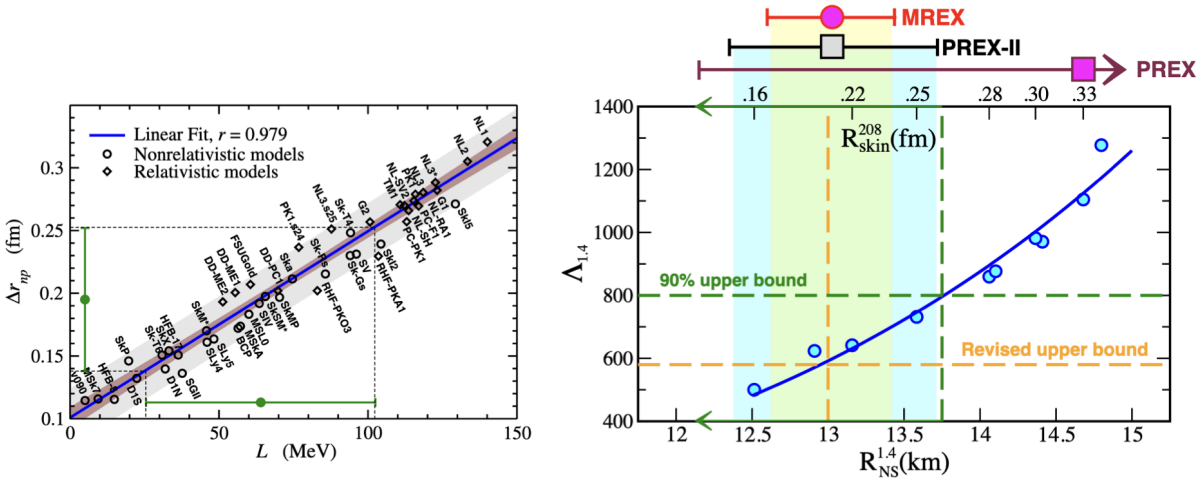

Figure 1: Left: Neutron skin of ^{208}Pb versus slope of the symmetry energy as calculated with various nuclear models: the correlation between the two is found to be quite stable [2]. Right: Constraints provided on density functional theory by combining the tidal polarizability parameter ($\Lambda_{1.4}$) of GW170817 observed by the LIGO-Virgo collaboration [3] and their more recent analysis [4] together with present and future ^{208}Pb neutron-skin measurements [5].

The first direct detection of gravitational waves from the coalescence of a binary neutron star system on August 17, 2017 (GW170817) by the LIGO-Virgo collaborations [3] has opened up a new window into the study of neutron-rich matter under extreme conditions. First calculations of the tidal deformability parameter of two spiraling neutron stars as a function of the neutron-skin thickness of ^{208}Pb and neutron star radius within different density functional models have been

performed (Fig. 1, right plot). Of course, such correlations are only approximate, however, they indicate quite a general behaviour: the higher the pressure at low density the larger the skin and the higher the pressure at higher densities the bigger the deformability.
Recently, first results for PSR J0030+0451 from the NASA observatory Neutron Star Interior Composition ExploreR (NICER) [6] put additional constraints on the mass-radius relation of neutron stars and, thus, on the EoS. More accurate constraints are expected both from LIGO/Virgo future O4 and O5 campaigns as well as from newest data of NICER on heavy neutron stars of known masses.
Even stronger constraints on the EoS can be imposed by combining the information on the neutron-skin thickness from terrestrial measurements with astronomical observations (see right plot of Fig. 1). In order to consistently compare the newest data coming from the emergent multi-messenger astronomy field with terrestrial measurements, it is imperative to constrain the systematic and model dependent uncertainties on the extraction of the neutron-skin thickness.
In spite of the increasing experimental effort to determine the neutron-skin thickness of nuclei, a precise measurement of this quantity still remains elusive. Determining the neutron radius of a nucleus is complex: bulk neutron densities cannot be directly probed in electron scattering experiments because the neutron is uncharged. Various techniques have been used to extract this critical observable: these range from hadron scattering experiments (involving protons, antiprotons and pions), electric dipole polarizabilities (EDP), pygmy dipole resonances (PDR), and coherent pion photoproduction among others (see [5] and references therein). These data are valuable but, unfortunately, are plagued by considerable model dependencies and uncontrolled uncertainties.
As exemplary case, the reported precision on the neutron skin from coherent π^0 photoproduction [7] has been a matter of intense debate within the community since the result was first published in 2014: while the experimental error in the determination of the cross section may be realistic, it has been argued that the theoretical error is grossly underestimated due to various contributions that were either underestimated or ignored, such as pion charge exchange, accurate knowledge of the optical potential, non localities, and medium modifications of nucleon resonances. To further investigate the suitability of this technique to extract neutron-skin thicknesses, a novel combined experimental and theoretical effort has been undertaken in Mainz within the Collaborative Research Center 1044. The preliminary results indicate that the sensitivity of coherent neutral-pion photoproduction to the neutron-skin thickness is rather low [8, 9]. Thus, this process does not seem to be suited to the study of neutron-skin thicknesses. Direct measurements of the neutron rms-radius would have smaller model dependencies and therefore provide an important test of the systematic uncertainties. The least model dependent extraction of the neutron-skin thickness appears to be via parity-violation electron scattering (PVES) [5]. Indeed, PVES is particularly sensitive to the neutron density [10].
The parity-violating asymmetry A_{PV} is determined from the difference in cross sections between the scattering of right- and left-handed electrons:

$$A_{\mathrm{PV}} = \frac{\sigma_R - \sigma_L}{\sigma_R + \sigma_L}. \tag{3}$$

In the Born approximation A_{PV} is directly proportional to the ratio of the weak (F_{W}) to the charge (F_{ch}) form factors of the nucleus, quantities that are obtained as the Fourier transforms of their corresponding spatial densities [11]:

$$A_{\mathrm{PV}} \approx \frac{G_{\mathrm{F}} Q^2}{4\pi\alpha\sqrt{2}} \frac{Q_{\mathrm{W}}\, F_{\mathrm{W}}(Q^2)}{Z\, F_{\mathrm{ch}}(Q^2)}, \tag{4}$$

where G_{F} and α are the Fermi and fine structure constants, while Z and Q_{W} are the electric and weak charge of the nucleus, respectively.

Given that the charge form factor $F_{\mathrm{ch}}(Q^2)$ is known to high accuracy, the parity-violating asymmetry determines, at least in the Born limit, the weak form factor $F_{\mathrm{W}}(Q^2)$ at the four-momentum transfer of the experiment. By normalising $F_{\mathrm{W}}(Q^2 = 0)$=1 the weak-charge radius is then given by:

$$R_W^2 = -6\frac{dF_W}{dQ^2}\bigg|_{Q^2=0} . \tag{5}$$

The PREX experiment [11] at the Jefferson Laboratory (JLab) has demonstrated the feasibility of this method meanwhile outlining its major experimental challenges.

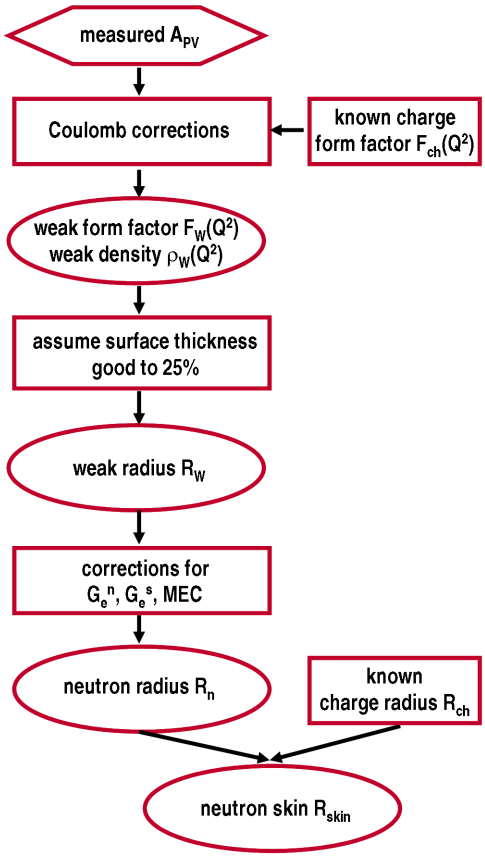

Figure 2: Flow chart illustrating the theoretical steps required to extract the neutron-skin thickness from the measured parity-violating asymmetry A_{PV}.

A new experimental campaign [12] aiming at a precision of $1\,\%$ on the neutron radius has been completed in fall last year and first results are expected for next year. In the near future at the Mainz Energy recovering Superconducting Accelerator (MESA) the weak mixing angle at low energy will be measured with unprecedented precision [13]. The same experimental setup will allow the measurement of the neutron radius of ^{208}Pb with a $0.5\,\%$ (or ± 0.03 fm) precision. Although the maximum incident energy at MESA will be lower than at JLab, the experiment will benefit from both higher beam intensities and full azimuthal coverage.

The ultimate precision on the neutron radius measurement at MESA will be limited by the implicit model assumption in the method on the surface thickness (see Fig. 2). The extraction of the neutron-skin thickness in PVES is indeed based on the measurement of the weak form factor at a single value of momentum transfer. Thus some assumptions concerning the surface thickness have to be made in order to reliably extract the neutron-skin thickness.

In order to remove this model dependence a determination of the surface thickness is necessary with a precision better than the current model assumption ($25\,\%$). In particular since the parity-violation asymmetry measurement at MESA will determine the neutron radius of ^{208}Pb with a precision of ± 0.03 fm the surface thickness must be known down to $10\,\%$.

Motivated by these new prospects we have recently performed, within the second funding period of the CRC1044, a variety of promising first experimental studies to address the feasibility of a wider program at the Mainz Mikrotron MAMI [14].

In particular we have performed an extensive study of the beam-normal single spin asymmetries A_{n} (so called transverse asymmetry) on medium-heavy nuclei. The choice has been driven by the fact that on one side such asymmetries are larger than the parity-violating ones (thus they are particularly suited for a commissioning of a new setup). On the other side their knowledge is mandatory in order to constrain the systematic error from a possible small normal component of the beam polarization in parity-violation experiments. This contribution will

become even more crucial for future experiments [13, 15, 16] aiming at a precision much higher than ever attained before.
Moreover, such measurements provide themselves an interesting challenge for theoretical predictions, requiring calculation of box diagrams with intermediate excited states.
So far, the transverse asymmetry at forward angles ($\theta < 6^\circ$) has been measured at JLab on ^{1}H, ^{4}He, ^{12}C, and ^{208}Pb [17]. A comparison to available theoretical calculations [18] showed a good agreement with the data except for ^{208}Pb: this striking disagreement has been a matter of debate in the community since its publication.
To that purpose a comprehensive experimental program to investigate beam-normal single spin asymmetries [19, 20] has been carried out at MAMI combining the high precision A1 spectrometers [21] and the DAQ electronics, beam monitoring and stabilization of the A4 collaboration [22–25]. It has laid an excellent basis for a significant near-future nuclear parity-violation measurement program, combining the existing expertise both in nuclear physics and in parity-violation electron scattering experiments.
The polarized $570\,\mathrm{MeV}$ electrons were produced using a strained GaAs/GaAsP super lattice photocathode that was irradiated with circularly polarized laser light [26, 27]. The longitudinal spin of the electrons leaving the photocathode was rotated to transverse orientation (in the horizontal plane) using a Wien filter which is positioned between the $100\,\mathrm{keV}$ polarized electron source and the injector linac of the accelerator. The polarization vector was finally rotated to vertical orientation using a pair of solenoids, located close behind the Wien filter. The orientation of the electron beam polarization vector was alternated between up and down by setting the high voltage of a fast Pockels cell in the optical system of the polarized electron source.
Since the MAMI accelerator so far had not been used to provide a vertically polarized beam, it is not equipped with a polarimeter capable of measuring the vertical polarization component directly. A new procedure has been applied to orient the electron polarization vector vertically, and a new sophisticated method has been developed to determine both its magnitude and orientation with the available setup [28]. This was accomplished using a Mott polarimeter [29]

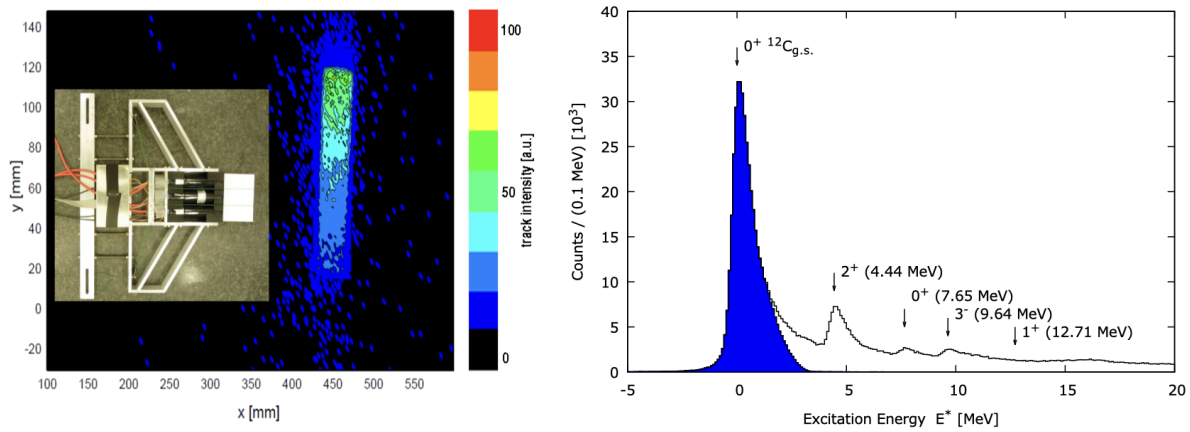

Figure 3: Left: Focal plane coordinate system of the high-resolution magnetic spectrometer (SpecA). Only coincidence events from the VDC and the PV-detector are shown. The insert shows the PV-detector consisting of three PMTs attached to a fused-silica bar. Right: The excitation energy spectrum of ^{12}C shows the acceptance of the spectrometer without (black line) and with (filled areas) a cut on the PV-detector.

downstream of the $3.5\,\mathrm{MeV}$ injector linac and a Møller polarimeter [28] close to the interaction point in the spectrometer hall. The degree of the vertical polarization was deduced by subtracting the horizontal polarization components from the total polarization.
For the measurements of the transverse asymmetry a $20\,\mu\mathrm{A}$ continuous-wave beam of verti-

cally polarized electrons was impinging on a $2.27\,\mathrm{g/cm^2}$ ($1.17\,\mathrm{g/cm^2}$, $1.11\,\mathrm{g/cm^2}$) ^{12}C (^{28}Si, ^{90}Zr) target.
Two newly built Cherenkov detectors (PV-detectors, see insert of Fig. 3, left plot), consisting of fused-silica bars ($300 \times 10 \times 50\,\mathrm{mm^3}$ and $100 \times 10 \times 50\,\mathrm{mm^3}$ adapted to the focal plane geometry of the spectrometers) read out via nine and three photomultiplier tubes respectively, were installed in the focal plane of the high resolution magnet spectrometers (SpecA and SpecB). The focus of the detector design lay on a high detection efficiency combined with a high rate capability. The PV-detector can be operated in two different modes: in the low current mode the full amplification range of the PMTs was exploited. Here, the PV-detectors are read out together with the spectrometer detectors. This setup allowed to make use of the high precision tracking detectors of the spectrometer, to perfectly align the PV-detectors on the elastic line of the scattered electrons by changing the magnetic field settings (Fig. 3, left panel shows the two dimensional histogram and the right panel the corresponding excitation energy spectrum). This was done with a low beam current of approximately $50\,\mathrm{nA}$. For the high beam current data

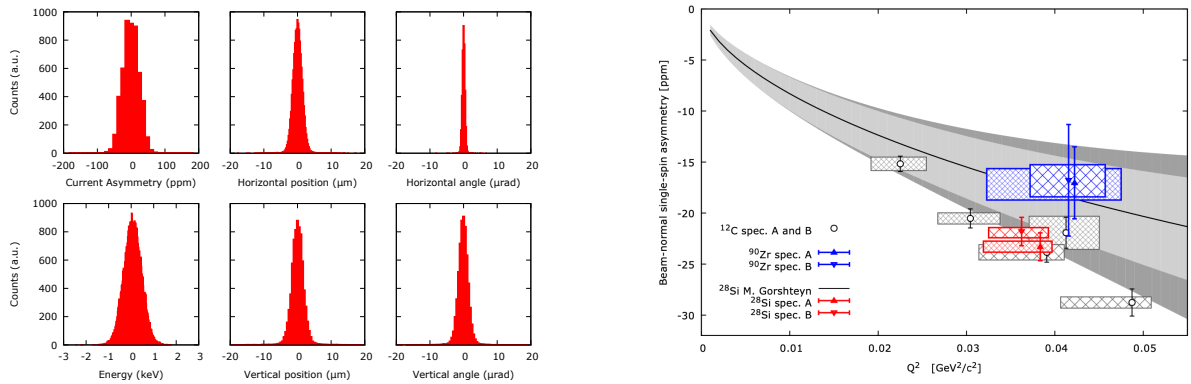

Figure 4: Left: Beam parameters after stabilization. Right: Extracted transverse asymmetries as a function of Q^2 for ^{12}C (open circles), for ^{28}Si (red triangles) and for ^{90}Zr (blue triangles). The width of the given boxes indicates the full width at half maximum of the Q^2 distribution. The statistical and systematic uncertainties are given by the error bars and the height of the boxes, respectively. The theoretical calculation is shown for comparison. The given bands belong to the uncertainty of the Compton slope parameter of $10\,\%$ (light grey) and $20\,\%$ (dark grey).

taking the tracking detectors were deactivated to protect them from radiation damage and the amplification of the PMTs was reduced to avoid a non-linear behavior. This was achieved by modifying the voltage dividers to allow for limiting the gain by disconnecting the last dynodes with an arrangement of relays.
The signals of the PMTs were integrated over a time window of $20\,\mathrm{ms}$ and read out using parts of the electronics of the former A4 experiment [22–25]. In addition to the detector signals, the signals from two X-Y-position monitors, an intensity monitor and an energy monitor as well as a constant current source have been acquired in order to reconstruct the beam position, relative angle, current, energy, and the integration gate length (see Fig. 4 left panel). All the information from the beam monitors as well as from the PV-detectors were combined in one data package. A feedback from the monitors to a stabilization system allowed the minimization of beam fluctuations correlated to the polarity changes.
A halfwave-plate in the laser system of the polarized source allowed to reverse the global polarization, and therefore invert the sign of the physical asymmetry. Two sets of data were taken: with halfwave-plate moved in (GVZIN) and moved out (GVZOUT). Comparing these results confirmed that the influence of the electric signal controlling the polarity reversal on the asymmetry measurement is negligible.

The experimental results have been compared to a theoretical calculation that relates the beam-normal single spin asymmetry to the imaginary part of the two-photon exchange amplitude [19] (see Fig. 4 right panel). Within the estimated theoretical uncertainty due to the unknown Compton slope parameter of $20\,\%$, the measurements are in agreement with the theoretical prediction. A dramatic disagreement, as it was obtained for ^{208}Pb [17], has not been observed for ^{90}Zr: though our result is affected by a large statistical uncertainty, its value is not compatible with zero, unlike for the ^{208}Pb measurement.

1.2 Project-related publications

1.2.1 Articles published by outlets with scientific quality assurance, book publications, and works accepted for publication but not yet published.

1. **Neutron skins of atomic nuclei: per aspera ad astra**
   M. Thiel *et al.*, J. Phys. G: Part. Phys., **46**, 093003 (2019).

2. **A future high-precision measurement of the weak mixing angle at low momentum transfer**
   D. Becker *et al.*, Eur. Phys. J. A **54**, 208 (2018).

3. **First measurement of the Q^2 dependence of the beam-normal single spin asymmetry for elastic scattering off Carbon**
   A. Esser *et al.*, Phys. Rev. Lett., **121**, 022503 (2018).

4. **Vertical beam polarization at MAMI**
   B. S. Schlimme *et al.*, Nucl. Instrum. Meth. A **850**, 54 (2017).

1.2.2 Other publications, both peer-reviewed and non-peer-reviewed

5. **Beam-Normal Single Spin Asymmetry for Elastic Scattering off Si and Zr**
   A. Esser *et al.*, arXiv:2004.14682 (submitted for publication to Phys. Lett. B).

6. **Development of an accurate DWIA model of coherent π^0 photoproduction to study neutron skins in medium heavy nuclei**
   F. Colomer *et al.*, under publication in J.Phys.Conf.Ser.,Contribution to the 27^{th} International Nuclear Physics Conference (INPC) 2019.

7. **Neutron skin studies in heavy nuclei with coherent π^0 photo-production**
   M.I. Ferretti Bondy *et al.*, PoS (Bormio2015) 008.

8. **From deep inside to outer space: exploring neutron skins**
   M. Thiel *et al.*, PoS (Bormio2015) 025.

9. **Neutron skin studies of medium and heavy nuclei**
   M. Thiel *et al.*, EPJ Web Conf. **73** (2014) 07007.

10. **Status and prospects of R_n measurements at Mainz**
    C. Sfienti *et al.*, AIP Conf.Proc. 1563 (2013) 1, 231.

Publications 1-8 (9-10) are based on work funded by the DFG within the CRC1044 in its second (first) funding period.

2 Objectives and work program

2.1 Anticipated total duration of the project

The anticipated total duration of the project is three years.

2.2 Objectives

The objectives of the of project will be:

1. **Transverse Asymmetry Measurements on ^{208}Pb**
   The beam-normal single spin asymmetry of ^{208}Pb will be measured at MAMI at two different beam energies in the energy regime of the future MESA accelerator. These data will allow on one side to benchmark the energy dependence of the beam-normal single spin asymmetry in the theoretical treatment. Together with the new measurement of A_{n} for ^{208}Pb by the PREX-II experiment [12] at substantially higher energy, they might provide on the other side additional clues to the solution of the current tension.

2. **Determination of the Surface Thickness of ^{208}Pb**
   For the first time the surface thickness of ^{208}Pb will be determined in parity-violation electron scattering at MAMI. Because of the current model uncertainty of $25\,\%$ (see Fig. 2) the precision in both the PREX-II and MESA neutron-skin determinations will be limited by this uncertainty. An independent $10\,\%$ measurement of the surface thickness will reduce this contribution to a level below the error budget of the parity-violation asymmetry measurement.
   These data will thus remove the dominant model dependence in the method and together with the newest PREX-II data they will provide the most stringent model independent measurement of the neutron-skin thickness in ^{208}Pb. This will pave the way to the most precise determination of the neutron-skin thickness at MESA.

3. **Publication of the results**
   Both analyses will be published in high ranking peer-reviewed journals and they will be presented during national and international conferences.

2.3 Work programme incl. proposed research methods

In order to fully achieve the objectives of this research proposal, a number of different working packages (WP) have been identified, which will be described here in more detail. The corresponding milestones are summarized in 2.3.7.

2.3.1 WP 1: Electronic Development

As outlined in 1.1 the previously used electronics had originally been built for the A4 parity-violation measurement. This setup was intended for the read-out of very high rate luminosity monitors. For this purpose, the current of the PMTs was integrated by analog electronics. For lower rate signals ($< 10\,\mathrm{MHz}$) this method becomes prone to baseline noise.
While the basic concepts of the measurement, such as the polarization reversal synchronized to the power grid frequency and the pseudo-random sequence of the polarization states in patterns of (+ - - +) and (- + + -) will be kept, most of the old electronics will be replaced by a state

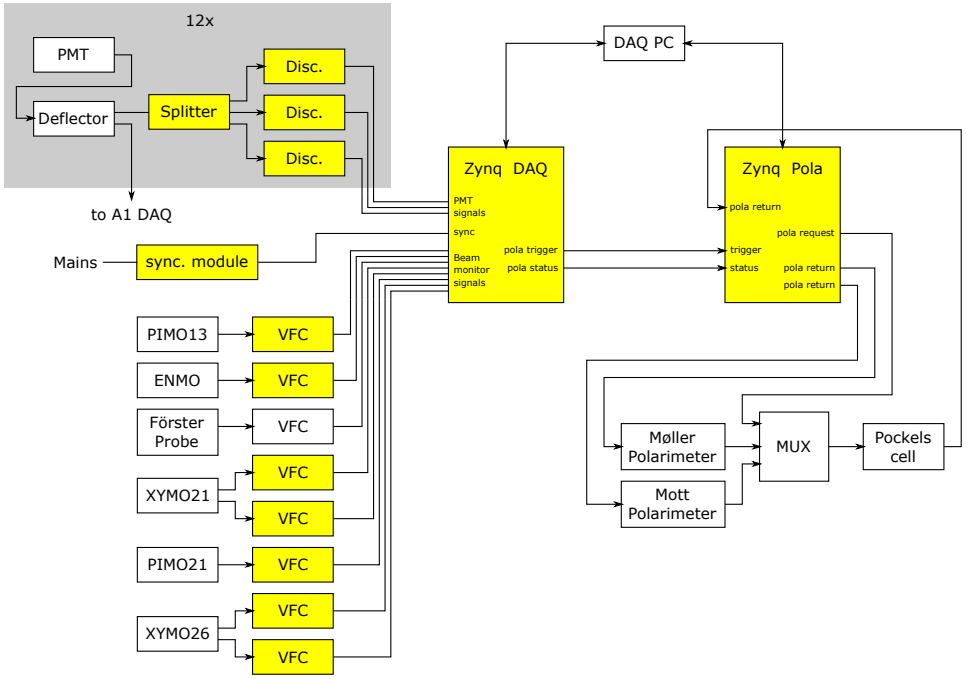

Figure 5: Schematic drawing of the planned electronic setup. The yellow components will be newly designed, while the white ones are already existing.

of the art system, fulfilling the requirements of the experiment.
The planned electronic setup will be centered around two Zync SoC (System on a Chip) boards, comprising an ARM processor used for experiment control and data read-out and a programmable logic (PL) used to implement fast digital logic circuits. A sketch of this setup is displayed in Fig. 5. One of the boards serves as data acquisition (DAQ), while the other one controls the beam polarization reversal. The PMT signals of both Cherenkov detectors will be connected to a set of discriminators allowing to acquire the counts with different thresholds simultaneously. The analog signals from the beam monitors will be converted to digital pulses by voltage to frequency converters (VFC) close to the individual monitor. The output pulses of the discriminators and VFCs will be counted by the Zynq DAQ board.
The other Zynq board will set and monitor the polarization direction at the beam source. This setup assures, that the information of the beam helicity for an individual integration gate is only stored near the beam source and can therefore not interfere with the DAQ electronics.
On the hardware side, PCBs will be designed for the voltage frequency converters and the discriminator chips. Input/output boards for level conversion and electric decoupling will be built for both Zync boards.
In the programmable logic of the DAQ-Zync board, the main feature which will be implemented are several high rate capable counters for acquisition of the digitized data.
On both Zync boards, computer programs will handle data acquisition and control of the beam polarization, and will transmit the data to the DAQ computer. A software will be developed to combine the data streams and save them locally.
Since hard- and software will run independently from other A1 experiments, the beam monitoring capability can be tested parasitically during other beam times, thus eliminating the need for dedicated beam tests.

2.3.2 WP 2: Target Cooling and Vacuum Sealing

The ^{208}Pb target needs to be cooled to prevent it from melting. A liquid cooling system for solid state targets is available from the previous measurements, therefore only a mounting frame for the lead target onto the cooling frame needs to be constructed.
Previous experiments have confirmed, that due to very high radiation levels close to the beam intersection point, rubber seals of the scattering chamber become brittle and therefore less tight within several days. Especially for high Z targets such as lead, this will limit the maximum duration of the experiment. To prevent this, a new scattering chamber, which has recently been constructed, was designed to accept spring energized metal seals which are much less prone to radiation damage. These seals need to be ordered and tested in the large opening for the scattering chamber windows.
The new scattering chamber was originally intended for a gas jet target. To extend its usage to solid state targets, a mechanism for changing targets will be constructed.

2.3.3 WP 3: Transverse Asymmetry Measurements on ^{208}Pb

The beam-normal single spin asymmetry A_n of ^{208}Pb will be measured using the same setup as described in 1.1 with the newly developed read-out electronics described in WP 1. The target will consist of a $0.57\,\mathrm{g/cm^2}$, isotopically enriched ($99.3\,\%$) ^{208}Pb foil which corresponds to $0.1\,X_0$ (radiation length).
To determine the energy dependence of the transverse asymmetry we propose to perform three measurements: two at $570\,\mathrm{MeV}$ and one at $210\,\mathrm{MeV}$. Both measurements at $570\,\mathrm{MeV}$ will be performed successively in one experimental campaign. An overview of the running conditions is listed in Tab. 1.

No.	$\mathbf{E_{Beam}}$	$\mathbf{I_{Beam}}$	$\mathbf{Q^2}$ ($\mathbf{GeV^2/c^2}$)		Stat. Uncertainty	Running Time
			SpecA	SpecB		
1	570 MeV	20 µA	0.04	0.04	2 ppm	10 days
2	570 MeV	20 µA	0.04	0.02	1 ppm (6 ppm)	2 days
3	210 MeV	20 µA	0.01	0.01	0.5 ppm	2 days

Table 1: Main parameters for the measurement of the energy dependence of the transverse asymmetry. In No. 2 the statistical uncertainty of 1 ppm refers to the low Q^2 measurement with SpecB (inside parentheses the corresponding uncertainty for the additional measurement with SpecA as indicated).

Measurement 1: symmetric Q^2 measurement at $570\,\mathrm{MeV}$
Beam-quality and setup have been already optimized for the measurement at $570\,\mathrm{MeV}$ during the various experimental campaigns previously performed.
For the symmetric Q^2 measurement, both PV-detectors will cover the same four-momentum transfer of $Q^2 = 0.04\,\mathrm{GeV^2/c^2}$. This is fundamental for the identification of possible instrumental asymmetries due to helicity-correlated changes of the beam parameters.
This measurement will provide the ultimate test of the newly developed electronics, and an extension of our mass dependence study of A_n (see Fig. 4, right plot).
The measurement aims for a determination of A_n with a statistical uncertainty of $2\,\mathrm{ppm}$. Here, 10 days of beam time are required.

Measurement 2: low Q^2 measurement at $570\,\mathrm{MeV}$
The second measurement at $570\,\mathrm{MeV}$ will be performed during the same experimental campaign as Measurement 1. While the PV-detector in spectrometer A will continue measur-

ing the transverse asymmetry at $Q^2 = 0.04\,\mathrm{GeV}^2/\mathrm{c}^2$, spectrometer B will be moved to $Q^2 = 0.02\,\mathrm{GeV}^2/\mathrm{c}^2$. This additional measurement at 570 MeV has two objectives. On one side the measurement with the Cherenkov detector in spectrometer A will further improve the statistical accuracy of the data point at $Q^2 = 0.04\,\mathrm{GeV}^2/\mathrm{c}^2$. On the other side the measurement at a lower Q^2 with spectrometer B will allow a more stringent benchmark of current theoretical calculations. Because of the large cross section at $Q^2 = 0.02\,\mathrm{GeV}^2/\mathrm{c}^2$, an accuracy of 1 ppm for A_n can be reached within 2 days.

Measurement 3: symmetric Q^2 measurement at 210 MeV
This energy range is of particular importance with regard to the upcoming ultimate determination of the neutron-skin thickness with the P2 detector setup at the MESA accelerator. Therefore a high-precision determination of A_n is mandatory.
However, the lower the beam energy, the larger the effort to maintain a high quality beam. Thus, it is essential to perform a symmetric Q^2 measurement in order to be sensitive to possible instrumental asymmetries. The experiment will be performed at $Q^2 = 0.01\,\mathrm{GeV}^2/\mathrm{c}^2$, the same four-momentum transfer as in the PREX-I/II experiments (both performed at an energy of 1.06 GeV). In addition to the determination of the energy dependence of the transverse asymmetry, this measurement can provide important findings with respect to the current tension between previous experimental results and the corresponding theoretical predictions. Because of the large cross section, a statistical uncertainty of 0.5 ppm can be achieved within 2 days of beam time.

2.3.4 WP 4: Determination of the Surface Thickness of the Weak-Charge Density of ^{208}Pb

To explore the sensitivity to the surface thickness, the weak density distribution $\rho_\mathrm{W}(r)$ is modeled with a two parameter Fermi function

$$\rho_\mathrm{W}(r, a, c) = \rho_0 \frac{\sinh c/a}{\cosh r/a + \cosh c/a}, \tag{6}$$

with the normalization constant ρ_0. The parameters a and c describe the surface thickness and the half-height radius of the nucleus, respectively. According to Eq. 6, one can write the radius R_W of the weak-charge distribution of ^{208}Pb as

$$R_\mathrm{W}^2 = \frac{1}{Q_\mathrm{W}} \int d^3r r^2 \rho_\mathrm{W}(r) = \frac{3}{5}c^2 + \frac{7}{5}\pi^2 a^2. \tag{7}$$

To calculate the sensitivity of the parity-violating asymmetry A_PV to changes in the surface thickness, R_W in Eq. 7 has to remain constant. Therefore both parameters a and c have to change. The sensitivity to a change in the surface thickness a is defined as

$$\varepsilon_\mathrm{a} = \frac{d \ln A_\mathrm{PV}}{d \ln a} = \frac{a}{A_\mathrm{PV}} \frac{dA_\mathrm{PV}}{da} \tag{8}$$

and it should be maximized.

The choice of kinematics for a measurement of the surface thickness with 10 % accuracy is guided by the goal of minimizing the running time of the experiment. Additional constraints concerning the experimental setup need to be taken into account as well. A comparison of the experimental settings and the necessary beam time is listed in Tab. 2.

According to the construction of the spectrometers and their arrangement on the pivot surrounding the scattering chamber, there are limitations in the accessible angular range. Furthermore, only selected beam energies at MAMI are equipped with a special stabilization system which is essential for performing parity-violation experiments.

Scenario 1:						
E_{Beam}	I_{Beam}	Scattering Angle θ		Four-Momentum Transfer Q^2		Running Time
		SpecA	SpecB	SpecA	SpecB	
855 MeV	20 µA	23.50°	10.35°	0.12 GeV^2/c^2	0.02 GeV^2/c^2	78 days
Scenario 2:						
E_{Beam}	I_{Beam}	Scattering Angle θ		Four-Momentum Transfer Q^2		Running Time
		SpecA	SpecB	SpecA	SpecB	
570 MeV	20 µA	24.4°	15.2°	0.06 GeV^2/c^2	0.02 GeV^2/c^2	166 days

Table 2: Running conditions for the two possible scenarios.

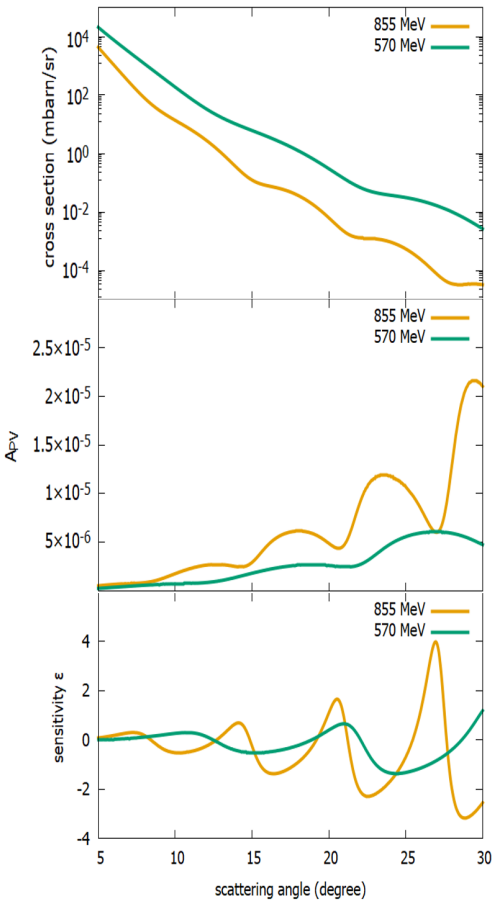

Figure 6: Cross section (top panel), parity-violating asymmetry A_{PV} (middle panel) and sensitivity ε of the asymmetry to changes in the surface thickness (bottom panel) as a function of the scattering angle θ for elastic scattering of electrons off ^{208}Pb at beam energies of 570 MeV (green) and 855 MeV (orange).

In Fig. 6 the results of the calculation for the sensitivity to the surface thickness in ^{208}Pb are shown for the two beam energies at which the stabilization of MAMI works and that are best suited for the aimed experiment. At forward scattering angles a measurement of the parity-violating asymmetry of ^{208}Pb has a reduced sensitivity to the surface thickness (see Fig. 6, bottom panel). While the sensitivity is increasing with the scattering angle, the cross section drops drastically (see Fig. 6, top panel).

To take into account the different behaviours of the three quantities shown in Fig. 6 in the optimisation process the figure of merit (FOM)

$$\mathrm{FOM} = \frac{d\sigma}{d\Omega} \cdot A_{\mathrm{PV}}^2 \cdot \varepsilon_{\mathrm{a}}^2. \qquad (9)$$

is computed.

The kinematics of the experiment is then chosen for a maximum of FOM thus reducing the total beam time needed to achieve the required accuracy. In addition the sensitivity of A_{PV} to the weak-charge radius must be suppressed w.r.t. the sensitivity to the surface thickness for the given beam energy and scattering angles.

The comparison of the two corresponding FOMs in Fig. 7 clearly shows that this is fulfilled for 855 MeV beam energy and spectrometer B placed at 10.35° as well as for 570 MeV beam energy and spectrometer B placed at 15.2°.

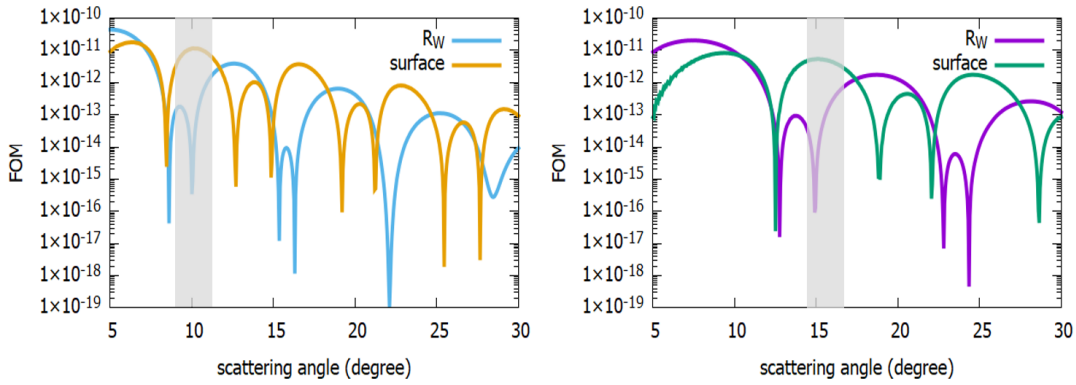

Figure 7: Comparison between the FOMs of the sensitivities to the surface thickness and to the weak-charge radius for 855 MeV (left panel) and 570 MeV (right panel). The grey area depicts the angular acceptance of spectrometer B.

A measurement at 855 MeV is the optimal choice to achieve the requested accuracy of $10\,\%$ within the shortest amount of time (78 days beam time are required). However such a measurement poses several experimental challenges. In order to access 10.35° with spectrometer B several major modifications to the experimental setup have to be made (see risk assessment in 2.3.6). This could require longer commissioning of the experimental setup and major delays due to higher radiation load in the experimental hall.

By contrast, the kinematics at 570 MeV is well tested and well-understood on grounds of our previously performed A_n studies. Here, no major construction work is necessary in order to perform the experiment. However, due to the lower cross section, the running time will be about twice longer compared to the 855 MeV measurement.

For both investigated scenarios, the Cherenkov detector in spectrometer A will be used to measure the weak form factor $F_\mathrm{W}(Q^2)$ at a higher Q^2 value. Because of the lower cross section, this measurement will be less precise in the given time period, but it will provide a second experimental anchor of the weak form factor to benchmark theoretical predictions. For the measurement of the weak form factor, it is necessary to reduce the angular acceptance of the PV-detector placed in spectrometer A in order to narrow the momentum transfer range of $F_\mathrm{W}(Q^2)$ yielding a more precise result.

Based on the long running time, the experimental campaign needs to be divided into several beam-time blocks of three weeks each. Due to possible contributions of the normal component in the polarization vector, each beam time has to include a measurement of the transverse asymmetry A_n.

2.3.5 WP 5: Analyses and Publications

The novel method of performing parity-violation experiments by counting individual scattered electrons with the developed electronics system (WP 1) will be published in a peer-reviewed journal specialized on instrumentation.

For the analysis of the data of WP 3 all the tools and coding is well-proven and ready for operation. Hence, the obtained results are expected to be published in a high ranking peer-reviewed journal shortly after the end of both experimental campaigns.

The tools and coding used for the analysis of the transverse asymmetry can be also used for the analysis of the data of WP 4 with respect to the extraction of the parity-violating asymmetry. Due to the long running time of the entire experiment, it will be subdivided into several beam time blocks. Here, the data of each block can be analyzed separately and the individual results

can be combined at the end.
We are aiming for a publication of this important result in a high ranking peer-reviewed journal. Given that the collection of the required statistics will last until almost the end of the applied funding period, we will be able to submit the paper until the end of year three, but to finish the complete publication process seems to be unlikely due to the time constraints of the project.

2.3.6 Risk Assessment

Electronics
Even though the electronic setup will be novel for this kind of experiment, the project group is experienced in working with the different types of components and it is constantly supported by the electronics workshop of the Institute of Nuclear Physics. The digitization of analog beam monitor signals already works reliably for the Förster probe proving the feasibility of this approach.
The only critical part of the new design lies in the PMT signal discriminators, which need to work at very high rates. However, based on our experience the asymmetry measurement can tolerate signal pileup up to a certain extent, as long as the detectors are frequently calibrated. If in the case of ^{208}Pb the pileup level should exceed the maximum which calibrations can account for, the signal will be integrated as it is currently the case.
Thus, the overall risk connected with WP1 is to be considered negligible.

^{208}Pb target
The low melting temperature of ^{208}Pb ($\approx 600\,\mathrm{K}$) in combination with the use of a high-intensity electron beam represents a rather high risk of melting the target during the experiment. To protect the lead target, several measures are foreseen. The beam spot will be scanned over an area of $4\,\mathrm{mm} \times 4\,\mathrm{mm}$ for a better distribution of the heat load. Moreover, the target foils will be placed inside a cooling frame, which was already operated successfully for a natural lead target during a test beam time.
However, according to the experience gained by the PREX collaboration in performing high-precision and high-intensity PV experiments with ^{208}Pb, it is expected, that – despite all protective measures – the target material will be most likely damaged after a time scale of approximately four weeks. To assure high-quality data taking during the entire experimental campaign, altogether three ^{208}Pb target foils will be mandatory. By mounting all three targets in the cooling frame in the scattering chamber, the production target can be easily exchanged as soon as the actual target foil starts degrading due to temperature overload.

Thereby the risk of a target damage gets minimized and it is guaranteed, that the resulting systematic uncertainty due to density fluctuations of the target material is kept within the required limits.

Measurement of the Transverse Asymmetry
The measurement of the transverse asymmetry at various beam energies will complete our studies in this field. The experimental setup as well as the explored kinematic region is well-known and understood. A low to medium risk is connected with the experiment at the lowest beam energy ($210\,\mathrm{MeV}$) because of possible halo contamination in the primary beam arising from the smaller number of turns in the microtron. On the other side novel improvements in the accelerator have recently shown that such contamination can be kept to a minimum.

Thus the overall risk of WP 3 is negligible.

Determination of the Surface Thickness
While Scenario 1 is clearly to be favored because of its shorter running time, the risks connected are higher compared to Scenario 2. The need to move one of the spectrometers to

more forward angles will force the use of a smaller beam pipe. This might cause an increase in radiation level in the experimental hall. The spread of radiation inside the smaller exit beam pipe has been studied using the simulation tool FLUKA. Although the results look promising, the risk still remains that the given safety limits, especially those of the exhaust air, will be exceeded. In addition, the necessary new design of the scattering chamber – to access 10.35° with spectrometer B – poses a challenge for the construction of the large-area windows, thus for the metal seals.
The measurement of Scenario 2 can be performed under well-known experimental conditions. Thus the determination of the surface thickness of ^{208}Pb can be performed without any major difficulties. However, due to the necessary amount of beam time in this case, the experimental campaign will extend until almost the end of the funding period.

Possible delays due to COVID-19
The University of Mainz is since early March 2020 in emergency operation mode and access to the infrastructure of the Institute of Nuclear Physics is permitted only in exceptional cases. We believe that the overall situation will improve in 2021 so that access to the institute will be granted and beam times at MAMI will again be available. Any delay w.r.t normal operation of the University (thus of the Institute of Nuclear Physics) from January 2021 will imply a one-to-one delay in the achievement of the different milestones of the project.

2.3.7 Schedule and Milestones

		2021				2022				2023			
Work Package	Milestone	I	II	III	IV	I	II	III	IV	I	II	III	IV
1	Electronic Development and Construction												
1	Test Experiment Electronic												
2	Test Experiment Scattering Chamber and Target												
5	Publication: Electronics												
3	Experiment: Transverse Asymmetry												
5	Analysis and Publication: Transverse Asymmetry												
4	Experiment: Surface Thickness												
5	Analysis and Publication: Surface Thickness												

Figure 8: Timeline and milestones for the proposed work packages. The dashed area in the milestone of WP 4 extending until end of the funding mirrors the risk associated to the measurement as described in 2.3.6

The timeline as well as the milestones for the proposed work packages are shown in Fig. 8 under the assumption that funding will begin in January 2021.
The development and construction of the new electronics system is the first milestone and is planned to be ready in summer 2021. Afterwards several test experiments are scheduled to debug the system. The experimental campaign on the transverse asymmetry will start at the beginning of the second year and contains several blocks of beam time. The associated analysis of the data will take place in parallel and will be completed with the publication of the results in the third quarter of 2022. The final milestones are the determination of the surface thickness with the associated publication of the results at the end of the third year.

3 Bibliography concerning the state of the art, the research objectives, and the work programme

References

[1] C.J. Horowitz *et al.*, J. Phys. G **41**, 093001 (2014).

[2] X. Roca-Maza *et al.*, Phys. Rev. Lett. **106**, 252501 (2011).

[3] P.B. Abbott *et al.*, Phys. Rev. Lett. **119**, 161101 (2017).

[4] P.B. Abbott *et al.*, Phys. Rev. Lett. **121**, 161101 (2018).

[5] M. Thiel *et al.* J. Phys. G: Part. Phys., **46**, 093003 (2019) - Project-related publications N.1 -.

[6] T. E. Riley *et al.*, Astro. J. Lett., **887**, L21 (2019).

[7] C. M. Tarbert *et al.*, Phys. Rev. Lett. **112**, 242502 (2014).

[8] M.I. Ferretti-Bondy, PhD thesis, University of Mainz (2020), to be published.

[9] F. Colomer, PhD thesis, University of Brussels (2020), to be published.

[10] C. Horowitz *et al.*, Phys. Rev., C **85**, 032501 (2012).

[11] S. Abrahamyan *et al.*, Phys. Rev. Lett. **108**, 112502 (2012).

[12] K. Paschke *et al.*, JLab PAC 38 - PREX-II ,https://hallaweb.jlab.org/parity/prex/prexII.pdf

[13] D. Becker *et al.*, Eur. Phys. J. A **54**, 208 (2018) - Project-related publications N.2 -.

[14] H. Herminghaus *et al.*, Nucl. Instrum. Meth. **138**, 1 (1973).

[15] J. Benesch *et al.*, arXiv:1411.4088.

[16] J. P. Chen *et al.*, arXiv:1409.7741.

[17] S. Abrahamyan *et al.*, Phys. Rev. lett. **109**, 192501 (2012).

[18] M. Gorchtein and C. J. Horowitz, Phys. Rev. C **77**, 044606 (2008).

[19] A. Esser *et al.*,Phys. Rev. Lett., **121**, 022503 (2018) - Project-related publications N.3 -.

[20] A. Esser *et al.*, arXiv:2004.14682 (submitted to Phys. Lett. B) - Project-related publications N.5 -.

[21] K. I. Blomqvist *et al.*, Nucl. Instrum. Meth. **A403**, 263 (1998).

[22] F. E. Maas *et al.*, Phys. Rev. Lett. **93**, 022002 (2004).

[23] F. E. Maas *et al.*, Phys. Rev. Lett. **94**, 082001 (2005).

[24] F. E. Mass *et al.*, Phys. Rev. Lett. **94**, 152001 (2005).

[25] S. Baunack *et al.*, Phys. Rev. Lett. **102**, 151803 (2009) .

[26] K. Aulenbacher *et al.*, Nucl. Instrum. Meth. **A391**, 498 (1997).

[27] K. Aulenbacher *et al.*, Eur. Phys. J. **ST 198**, 361 (2011).

[28] B. S. Schlimme *et al.*, Nucl. Instrum. Meth. **A850**, 54 (2017) - Project-related publications N.4 -.

[29] K. H. Steffens *et al.*, Nucl. Instrum. Meth. **A325**, 378 (1993).

4 Relevance of sex, gender and/or diversity

not applicable